Molecular Biology of the Cell
Vol. 18, 636–645, February 2007

Efficient Cargo Sorting by ESCRT-I and the Subsequent Release of ESCRT-I from Multivesicular Bodies Requires the Subunit Mvb12[D]

Matt Curtiss, Charles Jones, and Markus Babst

Department of Biology, University of Utah, Salt Lake City, UT 84112-9202

Submitted July 10, 2006; Revised October 26, 2006; Accepted November 20, 2006
Monitoring Editor: Sandra Lemmon

The endosomal sorting complex required for transport (ESCRT)-I protein complex functions in recognition and sorting of ubiquitinated transmembrane proteins into multivesicular body (MVB) vesicles. It has been shown that ESCRT-I contains the vacuolar protein sorting (Vps) proteins Vps23, Vps28, and Vps37. We identified an additional subunit of yeast ESCRT-I called Mvb12, which seems to associate with ESCRT-I by binding to Vps37. Transient recruitment of ESCRT-I to MVBs results in the rapid degradation of Mvb12. In contrast to mutations in other ESCRT-I subunits, which result in strong defects in MVB cargo sorting, deletion of *MVB12* resulted in only a partial sorting phenotype. This trafficking defect was fully suppressed by overexpression of the ESCRT-II complex. Mutations in *MVB12* did not affect recruitment of ESCRT-I to MVBs, but they did result in delivery of ESCRT-I to the vacuolar lumen via the MVB pathway. Together, these observations suggest that Mvb12 may function in regulating the interactions of ESCRT-I with cargo and other proteins of the ESCRT machinery to efficiently coordinate cargo sorting and release of ESCRT-I from the MVB.

INTRODUCTION

Eukaryotic cells continuously remove transmembrane proteins from the plasma membrane by endocytosis and deliver them to the lumen of the lysosome for degradation (for review, see Gruenberg and Stenmark, 2004; Katzmann *et al*., 2002). The topological problem of degrading transmembrane proteins in the lumen of the lysosome is solved by the formation of endosomal structures called multivesicular bodies (MVBs), which are formed by invagination and budding of vesicles from the limiting endosomal membrane into the lumen of the endosome. During this process, endosomal transmembrane proteins destined for degradation are sorted into forming vesicles and upon MVB fusion with the lysosome/vacuole, they are delivered to the lumen of the compartment, whereas others are maintained on the limiting membrane. A variety of studies indicate that monoubiquitination serves as a signal that directs protein cargo into the MVB pathway (Babst, 2005; Katzmann *et al*., 2002).

Sorting of endocytosed cell surface proteins through the MVB pathway plays an essential role in maintaining proper cell surface protein composition. In addition, this pathway acts to quickly and dramatically change the protein composition of the cell surface during processes such as differentiation and adaptation. For example, growth factor signaling is regulated in part by the controlled endocytosis and degradation of growth factor receptors, a process that is disrupted in pathological states of uncontrolled cellular proliferation in certain types of cancer (Di Fiore and Gill, 1999; Babst *et al*., 2000; Ceresa and Schmid, 2000; Thompson *et al*., 2005; Vaccari and Bilder, 2005). In addition to protein degradation, the MVB pathway also functions in the targeting and transport of lysosomal resident proteins. For example, in yeast the membrane-associated vacuolar enzyme carboxypeptidase S (CPS) is delivered from the *trans*-Golgi via MVBs to the lumen of the vacuole, the yeast organelle corresponding to the mammalian lysosome where it acts as a lumenal protease (Odorizzi *et al*., 1998). Thus, the MVB pathway also plays an important role in maintaining the function of the lysosomal/vacuolar compartment. Furthermore, MVBs have been shown to play an essential role in the immune response of mammals where they function in antigen presentation by dendritic cells and in the formation of exosomes (Murk *et al*., 2002).

Both MVB vesicle formation and sorting of ubiquitinated MVB cargo depends on the function of a group of at least 16 conserved proteins that were originally identified in the yeast *Saccharomyces cerevisiae* as class E vacuolar protein sorting (Vps) proteins (Babst, 2005). Deletion of each of the class E *VPS* genes in yeast results in the accumulation of endosomal cargo in large structures adjacent to the vacuole, called class E compartments (Raymond *et al*., 1992). This distinctive phenotype allows rapid identification of MVB sorting mutants in yeast. In addition to the morphological phenotype, in class E *vps* mutants transmembrane proteins such as CPS that are normally sorted to the vacuolar lumen are mislocalized to the limiting membrane of the vacuole (Odorizzi *et al*., 1998). Furthermore, the endosomal defects in class E *vps* mutants result in impaired transport of soluble vacuolar hydrolases from the *trans*-Golgi to endosomes, which ultimately leads to the secretion of a portion of the newly synthesized enzymes (Raymond *et al*., 1992).

This article was published online ahead of print in *MBC in Press* (http://www.molbiolcell.org/cgi/doi/10.1091/mbc.E06–07–0588) on November 29, 2006.

[D] The online version of this article contains supplemental material at *MBC Online* (http://www.molbiolcell.org).

Address correspondence to: Markus Babst (babst@biology.utah.edu).

Abbreviations used: ESCRT, endosomal sorting complex required for transport; MVB, multivesicular body; Vps, vacuolar protein sorting.

The majority of the class E Vps proteins are constituents of three separate hetero-oligomeric protein complexes called endosomal sorting complex required for transport (ESCRT)-I, ESCRT-II, and ESCRT-III and the Vps4 ATPase complex. The ESCRT protein complexes are transiently recruited from the cytoplasm to the endosomal membrane where they function in transmembrane protein sorting and the formation of MVB vesicles. The ESCRT-I protein complex is recruited to the MVB by Vps27, a class E Vps protein that localizes to the endosome by binding to the lipid phosphatidylinositol 3-phosphate (Bache *et al*., 2003; Katzmann *et al*., 2003). On the endosomal membrane both ESCRT-I and Vps27 bind to ubiquitinated endosomal cargo (Katzmann *et al*., 2001; Pornillos *et al*., 2002; Bilodeau *et al*., 2003; Swanson *et al*., 2003; Sundquist *et al*., 2004; Teo *et al*., 2004; Hirano *et al*., 2006). In addition, ESCRT-I interacts with ESCRT-II, which initiates the oligomerization of at least four small coiled-coil proteins, resulting in the formation of the ESCRT-III complex (Babst *et al*., 2002b; Teo *et al*., 2006). ESCRT-III is a large endosome-associated structure that seems to function in the concentration of MVB cargo (Babst *et al*., 2002a). After protein sorting has been completed, the multimeric AAA-type ATPase Vps4 binds to ESCRT-III and disassembles the ESCRT-III complex in an ATP-dependent manner (Babst *et al*., 1998, 2002a).

ESCRT-I is a 350-kDa protein complex that has been shown to be composed of the three class E Vps proteins: Vps23, Vps28, and Vps37 (Babst *et al*., 2000; Katzmann *et al*., 2001). However, expression of these subunits in *Escherichia coli* does not result in the formation of a 350-kDa complex, suggesting that additional unidentified subunits might be necessary for the formation of ESCRT-I in yeast (Kostelansky *et al*., 2006; Teo *et al*., 2006). In this publication, we present evidence for a fourth subunit of the yeast ESCRT-I complex, called Mvb12. Loss of Mvb12 results in a partial defect in MVB sorting and the mistargeting of ESCRT-I to the vacuolar lumen. These data suggest that Mvb12 is not an essential factor for ESCRT-I function but that it may be required for efficient cargo sorting and the release of ESCRT-I from the MVB.

MATERIALS AND METHODS

Materials

Monoclonal antibodies specific for the hemagglutinin (HA) epitope and green fluorescent protein (GFP) were purchased from Covance (Princeton, NJ). Polyclonal antisera against Snf7 (Babst *et al*., 1998) and Vps23 (Babst *et al*., 2000) have been characterized previously.

Strains and Media

S. cerevisiae strains used in this work are listed in Table 1. Yeast strains were grown in standard yeast extract-peptone-dextrose (YPD) or synthetic medium supplemented with essential amino acids as required for maintenance of plasmids (YNB) (Sherman *et al*., 1979). The deletion strains were constructed by transforming a yeast strain with a DNA fragment containing the *HIS3* or *URA3* gene flanked by 50 base pairs specific for the 5′ and 3′ region of the corresponding gene. Yeast cells were selected for the presence of the *URA3* or *HIS3* gene, and the deletions were confirmed by PCR analysis of the chromosomal DNA.

DNA Manipulations

Recombinant DNA work was performed using standard protocols (Sambrook *et al*., 1989). Transformation of *S. cerevisiae* was done by the lithium acetate method as described in Ito *et al*. (1983). The plasmids used in this study are listed in Table 1. The *MVB12* gene was obtained by polymerase chain reaction (PCR) amplification of SEY6210 chromosomal DNA and inserted into the EcoRI/BamHI sites of pRS416, resulting in the plasmid pMB238. For the construction of pMB240, pCJ2, and pMC26, a DNA fragment coding for three HA epitopes was ligated with PCR products containing either *MVB12* or *VPS37*, respectively, and inserted into BamHI/SalI-digested pRS416 or pRS426 vector. pMB239 and pMB306 were constructed by ligating a PCR product containing *MVB12* with a GFP-containing fragment from the vector pEGFP-C1 (Clontech, Mountain View, CA) into the BamHI/SalI sites of the vectors pRS416 and pRS426.

Experimental Procedures

For native immunoprecipitation experiments, 10 OD_{600} equivalents of yeast cells were spheroplasted and then osmotic lysed in 1 ml of phosphate-buffered saline (PBS) (8 g/l NaCl, 0.2 g/l KCl, 1.44 g/l Na_2HPO_4, and 0.24 g/l KH_2PO_4, pH 7.2) containing protease inhibitors. The resulting cell extracts were centrifuged at 15,000 × *g* for 5 min. The resulting supernatant was incubated with antibodies (1/250 anti-HA antibody) for 1.5 h at 4°C. The antibodies were isolated by adding GammaBind G-Sepharose (GE Healthcare, Little Chalfont, Buckinghamshire, United Kingdom). After incubation for 1 h at 4°C, the Sepharose was washed three times with PBS containing 0.5% Tween 20, and the antibodies together with the bound antigen were eluted by boiling the Sepharose in SDS-PAGE sample buffer. The resulting fractions were analyzed by SDS-PAGE and Western blotting. Vps23-ProtA was affinity purified from cell extract using IgG-Sepharose (GE Healthcare). Preparation of cell extract, incubation with the Sepharose, washes, and sample elution were performed as described for the immunoprecipitation experiments. Immunofluorescence microscopy was performed on fixed spheroplasted cells as described in Babst *et al*. (1998). Fluorescence microscopy was performed on a deconvolution microscope (DeltaVision, Applied Precision, Issaquah, WA). For gel filtration analysis, yeast cells were spheroplasted and lysed in PBS containing 0.1 mM 4-(2-aminoethyl)benzenesulfonyl fluoride and protease inhibitor cocktail (Complete; Roche Molecular Biochemicals, Indianapolis, IN). The lysate was centrifuged at 100,000 × *g*, and the resulting supernatant (~2 mg of protein) was loaded on a Sephacryl S300 column (16/60; GE Healthcare) and separated in presence of PBS. Subcellular fractionations were performed as described previously (Babst *et al*., 1997). Total cell extracts for Western blot analysis were obtained by glass bead lysis of yeast from 6 ml of culture (OD_{600} = 0.5) in SDS-PAGE sample buffer (2% SDS, 0.1 M Tris, pH 6.8, 10% glycerol, 0.01% bromphenol blue, and 5% β-mercaptoethanol).

RESULTS

Identification of Mvb12

A global analysis of protein localization in yeast identified a group of uncharacterized proteins that are localized to endosomal compartments (Huh *et al*., 2003). We tested the corresponding yeast deletion strains for phenotypes that are indicative of MVB mutations. Our studies identified the open-reading frame YGR206w as a factor required for the MVB sorting pathway (see phenotypic analysis in later sections of this article). YGR206w encodes a 12-kDa protein and therefore, we named this gene *MVB12*. Mvb12 is a basic protein (pI 8.35) that contains no obvious structural motifs and evolutionarily is poorly conserved. No clear *MVB12* homologues are identified in higher eukaryotes. Sequence homology searches identify uncharacterized open-reading frames in other genomes of fungal species as potential *MVB12* homologues. However, even among different yeast species the sequence conservation of Mvb12 is poor.

Mvb12 Transiently Localizes to MVBs

To study the localization of Mvb12, we constructed *MVB12-GFP*, a functional C-terminal GFP fusion of *MVB12* (Supplemental Figure 1). We expressed this fusion protein in different strains and analyzed these strains by fluorescence microscopy (Figure 1A). Consistent with the results of the global protein localization study, we observed that in wild-type cells Mvb12-GFP localized to the cytoplasm and to small compartments consistent with endosomes.

The AAA-type ATPase Vps4 functions in the dissociation of the ESCRTs from MVBs; therefore, mutations in *VPS4* result in the accumulation of the ESCRT machinery on aberrant endosomal membranes, the class E compartments (Figure 1A, arrows; Babst *et al*., 1998, 2002a). The deletion of *VPS4* resulted in the redistribution of Mvb12-GFP from the cytoplasm to larger compartments adjacent to vacuoles, consistent with class E compartments. Furthermore, by immunofluorescence microscopy we observed colocalization of Mvb12-GFP with the ESCRT-III subunit Snf7 in these cells, indicating that in *vps4*Δ Mvb12-GFP accumulates on endosomal compartments (Figure 1B). Interestingly, we observed

Table 1. Strains and plasmids used in this study

Strain or plasmid	Descriptive name	Genotype or description	Reference or source
S. cerevisiae			
BHY10	WT	SEY6210, *leu2-3, 112*::pBHY11 (CPY-Inv *LEU2*)	Rothman and Stevens (1986)
DKY48	*vps37*Δ	SEY6210, *VPS37::HIS3*	Katzmann *et al.* (2001)
DKY54	*VPS23-GFP*	SEY6210, *VPS23-GFP*, *HIS5* (*S. pombe*)	Katzmann *et al.* (2001)
DKY55	*vps4*Δ*/VPS23-GFP*	DKY54, *VPS4::TRP1*	Katzmann *et al.* (2001)
EEY5-2	*vps23*Δ	BHY10, *VPS23::HIS3*	This study
EEY6-2	*vps23*Δ	SEY6210, *VPS23::HIS3*	Babst *et al.* (2000)
EEY9	*snf7*Δ	SEY6210, *SNF7::HIS3*	Babst *et al.* (2002a)
GOY23	*pep4*Δ*/prb1*Δ	SEY6210, *PEP4::LEU2, PRB1::LEU2*	Luhtala and Odorizzi (2004)
JY138	*cim3-1*	*MAT*α *ade2-101 his*Δ*200 ura3-52 lys2-801 trp1*Δ*63 leu2*Δ*1 ADE2::TEL-VR adh4::URA3::TEL-VIIL cim3-1*	Mark Hochstrasser (Yale University, New Haven, CT)
MBY21	*vps27*Δ	SEY6210, *VPS27::HIS3*	Shih *et al.* (2002)
MBY22	*vps4*Δ*/vps27*Δ	MBY3, *VPS27::HIS3*	This study
MBY3	*vps4*Δ	SEY6210, *VPS4::TRP1*	Babst *et al.* (1997)
MBY30	*vps36*Δ	SEY6210, *VPS36::HIS3*	Babst *et al.* (2002b)
MBY55	*VPS36-GFP*	SEY6210, *VPS36-GFP*, *HIS5* (*S. pombe*)	Babst *et al.* (2002b)
MBY64	*mvb12*Δ*/vps4*Δ	MBY3, *MVB12::HIS3*	This study
MBY66	*mvb12*Δ	SEY6210, *MVB12::HIS3*	This study
MBY73	*mvb12*Δ*/VPS23-GFP*	DKY54, *MVB12::URA3*	This study
MBY74	*vps4*Δ*/mvb12*Δ*/VPS23-GFP*	DKY55, *MVB12::URA3*	This study
MCY38	*VPS36-GFP/mvb12*Δ	MBY55, *MVB12::URA3*	This study
MCY18	*vps4*Δ*/vps23*Δ	MBY3, *VPS23::HIS3*	This study
MCY19	*vps4*Δ*/vps37*Δ	MBY3, *VPS37::HIS3*	This study
MCY23	*vps28*Δ	SEY6210, *VPS28::HIS3*	This study
MCY25	*vps4*Δ*/vps28*Δ	MBY3, *VPS28::HIS3*	This study
MCY33	*pep4*Δ*/prb1*Δ*/mvb12*Δ	GOY23, *MVB12::HIS3*	This study
MCY9	*mvb12*Δ	BHY10, *MVB12::HIS3*	This study
SEY6210	WT	*MAT*α *leu2-3,112 ura3-52 his3-*Δ*200 trp1-*Δ*901 lys2-801 suc2-*Δ*9*	Robinson *et al.* (1988)
Plasmids			
pRS416		*URA3* Ap^R *CEN*	Christianson *et al.* (1992)
pGO45	GFP-CPS	*URA3* Ap^R (pRS426) *GFP-CPS1*	Odorizzi *et al.* (1998)
pCS24	Ste2-GFP	*URA3* Ap^R (pRS426) *STE2-GFP*	Odorizzi *et al.* (1998)
pMB175	2 μ ESCRT-II	*LEU2* Ap^R (pRS425) *VPS22-HA, VPS25, VPS36*	Babst *et al.* (2002b)
pMB238	*MVB12*	*URA3* Ap^R (pRS416) *MVB12*	This study
pMB239	*MVB12-GFP*	*URA3* Ap^R (pRS416) *MVB12-GFP*	This study
pMB240	*MVB12-HA*	*URA3* Ap^R (pRS416) *MVB12-HA*	This study
pMB142	*VPS23-ProtA*	*TRP1* Ap^R (pRS414) *VPS23-ProtA*	Katzmann *et al.* (2001)
pCJ2	*MVB12-HA*	*URA3* Ap^R (pRS426) *MVB12-HA*	This study
pEE23-10	*VPS23*	*TRP1* Ap^R (pRS414) *VPS23*	Babst *et al.* (2000)
pMB306	*MVB12-GFP*	*URA3* Ap^R (pRS426) *MVB12-GFP*	This study
pMC26	*VPS37-HA*	*URA3* Ap^R (pRS416) *VPS37-HA*	This study
pMB301	*HA-MVB12*	*URA3* Ap^R (pRS416) P_{CPS1} *HA-MVB12*	This study
pMB319	*VPS23(M85T)-GFP*	*TRP1* Ap^R (pRS414) *vps23-9-GFP*	This study
pMB320	*VPS23-RFP*	*URA3* Ap^R (pRS416) *VPS23-mCherry*	This study
pMB321	*MVB12-GFFP*	*URA3* Ap^R (pRS415) *MVB12-GFP*	This study
pDK*vps23-9*	*VPS23(M85T)*	*TRP1* Ap^R (pRS414) *vps23-9*	Katzmann *et al.* (2001)
pEE27-4	*GFP-VPS27*	*URA3* Ap^R (pRS416) *GFP-VPS27*	Katzmann *et al.* (2003)

that the endosomal accumulation of Mvb12-GFP in *vps4*Δ was dependent on the presence of Vps27 (Figure 1A). In *vps4*Δ*vps27*Δ cells, Mvb12-GFP localized mainly to the cytoplasm and a minor pool associated with smaller dispersed compartments. These compartments do not colocalize with Snf7, suggesting that they are not late endosomal structures (Figure 1B). Previous studies have shown that ESCRT-I localizes to the endosomal membrane by binding to Vps27 and that ESCRT-I accumulates on the membrane in a *VPS4* deletion strain (Bache *et al.*, 2003; Katzmann *et al.*, 2003). Therefore, our localization studies suggested that Mvb12 might be associated with ESCRT-I. This idea was further corroborated by the observation that red fluorescent protein (RFP)-tagged Vps23 and Mvb12-GFP colocalized in both wild-type and *vps4*Δ strains (Figure 1C). Furthermore, in strains deleted for the ESCRT-I subunit *vps37*Δ the fluorescent signal of Mvb12-GFP was dramatically reduced compared with other strain backgrounds (Figure 1A). This observation suggested that Mvb12-GFP is unstable in ESCRT-I mutants, a result consistent with Mvb12 being an ESCRT-I subunit.

Mvb12 Is a Subunit of the ESCRT-I Complex

To further study the effect of ESCRT mutations on the stability of Mvb12, we constructed a functional C-terminal HA-tagged Mvb12 (Mvb12-HA; Supplemental Figure 1) and expressed this fusion protein in wild type and mutant strain backgrounds. Cell extracts were prepared and analyzed for the presence of Mvb12-HA by Western blot (Figure 2A). The analysis of wild-type cells showed two specific bands, a major band at ~15 kDa that corresponds to the predicted molecular mass of Mvb12-HA (12 kDa for Mvb12 plus 3 kDa for HA-tag) and a minor band at ~20 kDa, which may be a

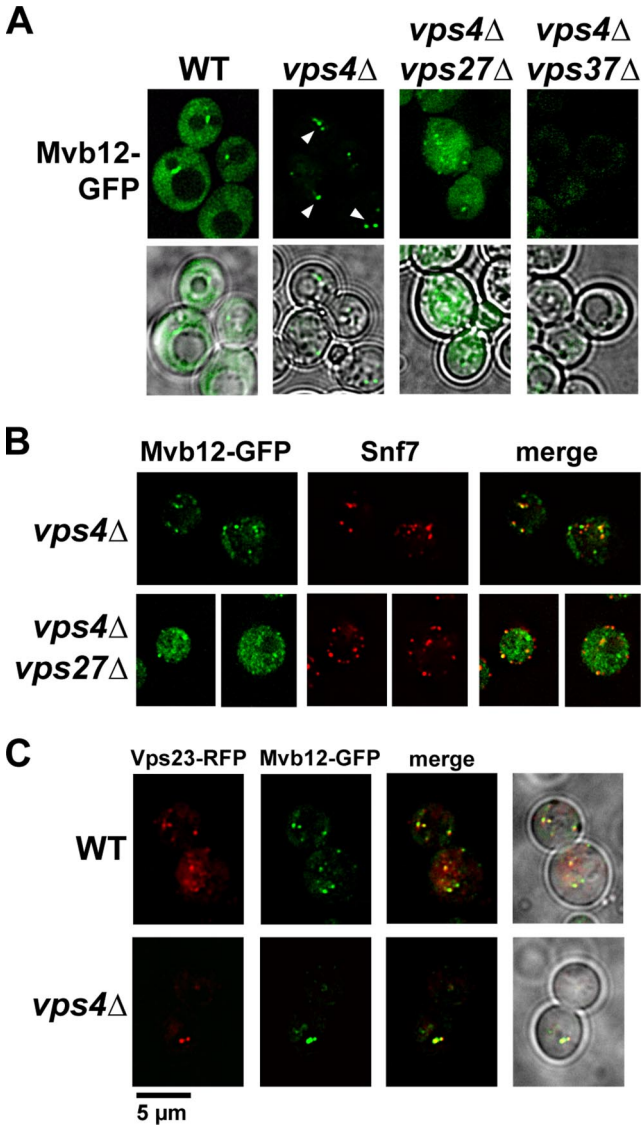

Figure 1. Localization of Mvb12 to MVBs is dependent on Vps27 and ESCRT-I. (A) Fluorescent microscopy of yeast strains (wild type [WT], MBY66; *vps4*Δ, MBY64; *vps4*Δ/*vps27*Δ, MBY22; and *vps4*Δ/*vps37*Δ, MCY19) expressing *MVB12-GFP* (pMB239). White arrows indicate class E compartments, aberrant endosomal structures present in class E *vps* mutants. (B) Immunofluorescence microscopy of *vps4*Δ (MBY3) and *vps4*Δ*vps27*Δ (MBY22) expressing *MVB12-GFP* (pMB239) demonstrates that colocalization of Mvb12 with endosome-associated ESCRT-III subunit Snf7 is dependent on Vps27. The Snf7 protein was visualized using specific anti-Snf7 antibody and fluorescently labeled secondary antibody. (C) Fluorescence microscopy of WT and *vps4*Δ (MBY3) strains expressing *VPS23-RFP* (pMB320) and *MVB12-GFP* (pMB321) demonstrates colocalization of Mvb12 with ESCRT-I.

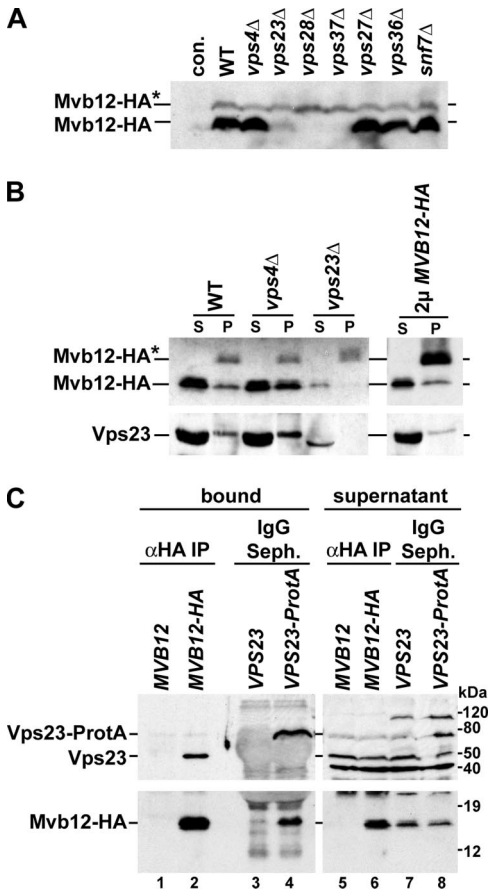

Figure 2. Mvb12 is unstable in ESCRT-I mutants and physically interacts with the ESCRT-I complex. (A) Western blot analysis using anti-HA antibodies of total cell extracts from yeast strains expressing *MVB12-HA* (pMB240) or as a negative control (con.) *MVB12* (pMB238). The strains used are described in Table 1. (B) Subcellular fractionation of yeast strains expressing *MVB12-HA* either from a low copy (pMB240) or a high copy (2μ, pCJ2) plasmid. The resulting supernatant (S) and pellet (P) fractions were analyzed by Western blot for the presence of Mvb12-HA and Vps23. (C) Extracts from wild-type cells expressing *MVB12* (negative control) or *MVB12-HA* were used for an immunoprecipitation experiment using anti-HA antibodies. Samples of the immunoprecipitated material (bound, lanes 1 and 2) and the remaining supernatants (lanes 5 and 6) were analyzed by Western blot for the presence of Mvb12-HA and Vps23. Extracts from wild-type yeast expressing *MVB12-HA* in addition to *VPS23* (negative control) or *VPS23-ProtA* were subjected to affinity purification by using IgG-Sepharose. The resulting enriched material (lanes 3 and 4) and the remaining supernatants (lanes 7 and 8) were analyzed by Western blot for the presence of Mvb12-HA and Vps23.

modified form of Mvb12-HA (Mvb12-HA*; Figure 2A). A similar band pattern was observed with cell extracts from strains deleted for *VPS4*, *VPS27*, *VPS36* (encoding an ESCRT-II subunit), and *SNF7* (encoding an ESCRT-III subunit). In contrast, cell extracts from the ESCRT-I mutant strains *vps23*Δ, *vps28*Δ, and *vps37*Δ exhibited a dramatically reduced amount of the major, 15-kDa band, confirming the observation by microscopy that Mvb12 is unstable in ESCRT-I mutants. However, the amount of the modified form of Mvb12-HA remained similar in all mutant strains (Figure 2A). To determine where this modification occurs, we studied the cellular distribution of Mvb12-HA and Mvb12-HA* by subcellular fractionation. For this purpose, we prepared cell extracts by spheroplasting and osmotic lysis and separated the extract by centrifugation at 15,000 × *g* into a soluble fraction (S) and a pellet fraction (P). Previous studies have shown that under these conditions, the MVB-associated protein pool is found in the pellet, whereas the cytoplasmic fraction remains in the supernatant (Babst *et al.*, 1998, 2002a). The Western blot analysis of the fractionation samples showed that in wild-type cells Mvb12-HA is mainly found in the soluble, cytoplasmic fraction, whereas in cells deleted for *VPS4* an increased amount of Mvb12-HA is observed in the membrane bound fraction (Figure 2B). These

results are consistent with the Mvb12-GFP localization observed by microscopy, although the redistribution to the membrane in *vps4*Δ is less pronounced than expected from the microscopy data (Figure 1A). Similarly, ESCRT-I has been shown by microscopy to accumulate on endosomal membranes in *vps4*Δ (Figure 7A; Katzmann *et al*., 2001); however, only a small portion of Vps23 is found in the membrane fraction of this strain (Figure 2B). A likely explanation for this discrepancy between the two methods is that during the fractionation procedure, peripheral proteins such as ESCRT-I might partially dissociate from the membrane.

As expected from our previous results, the deletion of the *VSP23* resulted in a reduced amount of Mvb12-HA in both the soluble and the pelletable pool (Figure 2B). In contrast to Mvb12-HA the amount and localization of the modified form Mvb12-HA* is not effected by the deletions of either *VPS4* or *VPS23*. In all strains, Mvb12-HA* is found exclusively in the pelletable fraction. This result suggested that the modification of Mvb12-HA might occur on the endosomal membrane and that the modified pool of Mvb12-HA may not be associated with ESCRT-I. This is further supported by the observation that in cells overexpressing Mvb12-HA, the majority of the protein is found in the pellet in the modified form (Figure 2B). The nature of the modification is not known. However, based on the size shift Mvb12-HA* could represent a phosphorylated or monoubiquitinated form of Mvb12.

These data are consistent with the model that Mvb12 is a subunit of the ESCRT-I protein complex. To further test this model, we studied a potential physical interaction between Mvb12 and ESCRT-I by immunoprecipitation experiments (Figure 2C). We prepared extracts from cells expressing either *MVB12* (negative control) or *MVB12-HA* and performed immunoprecipitations under native conditions by using anti-HA antibodies. The Western blot analysis of the resulting samples demonstrated the specific coimmunoprecipitation of Vps23 with Mvb12-HA (Figure 2C, lane 2). No Vps23 was immunoprecipitated from the Mvb12-containing control extract (Figure 2C, lane 1). A similar result was obtained by IgG-affinity purification. Cell extracts of strains expressing *MVB12-HA* together with *VPS23* or a functional protein A-tagged *VPS23* (*VPS23-ProtA*) were incubated with IgG-Sepharose, and the bound material was tested for the presence of Vps23 and Mvb12-HA. The data showed a specific copurification of Mvb12-HA with Vps23-ProtA (Figure 2C, lane 4), whereas no enrichment of Mvb12-HA was observed from the *VPS23*-expressing control extract (Figure 2C, lane 3). As a control for the presence of Mvb12-HA and Vps23 in the extracts, we performed Western blots of the supernatant after immunoprecipitation or affinity purification (Figure 2C, lanes 5–8). In summary, both immunoprecipitation and IgG-affinity purification experiments indicated a physical interaction between Mvb12 and ESCRT-I, supporting the notion that Mvb12 is a subunit of the ESCRT-I complex.

Finally, an extract from wild-type cells expressing *MVB12-HA* was separated on a gel filtration column, and the resulting fractions were analyzed by Western blot for the presence of Mvb12-HA and the ESCRT-I subunit Vps23. The results indicated a native molecular mass of ~350 kDa for Mvb12-HA similar to the size of ESCRT-I (as indicated by Vps23; Figure 3A, gels 1 and 2, and D). Furthermore, in a strain deleted for *MVB12* we observed a shift in the size range of the ESCRT-I subunits Vps23 and Vps37-HA to ~170 kDa (Figure 3A, gels 3 and 4, and D). Together, these protein interaction and gel filtration data strongly suggest that Mvb12 is a subunit of the ESCRT-I complex.

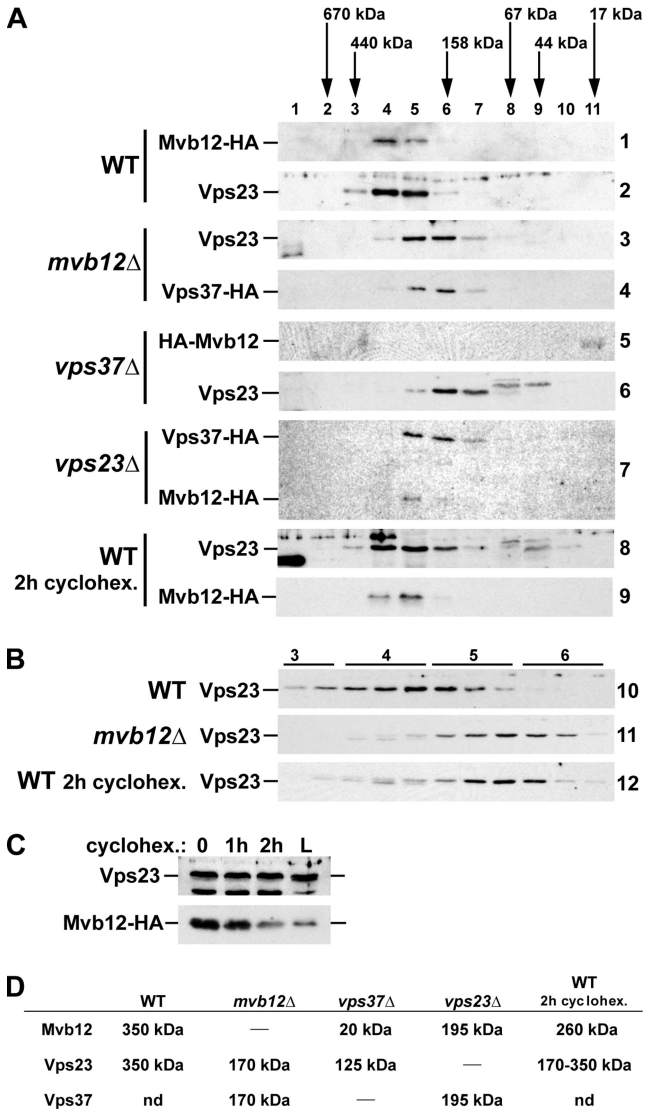

D

	WT	*mvb12*Δ	*vps37*Δ	*vps23*Δ	WT 2h cyclohex.
Mvb12	350 kDa	—	20 kDa	195 kDa	260 kDa
Vps23	350 kDa	170 kDa	125 kDa	—	170-350 kDa
Vps37	nd	170 kDa	—	195 kDa	nd

Figure 3. Gel filtration experiments suggest that Mvb12 associates with ESCRT-I via the subunit Vps37. (A) Cytosol from different yeast strains expressing either *MVB12-HA* (pMB240) or *HA-MVB12* (pMB301) was separated by gel filtration (Sephacryl S300), and the resulting fractions were analyzed by Western blot for the presence of Mvb12-HA, HA-Mvb12, and Vps23. Gels 8 and 9 show the results of the gel filtration analysis of wild type expressing *MVB12-HA* after 2 h of cycloheximide treatment. (B) Detailed analysis of gel filtration experiments from Figure 3A. Bars above the gels indicate the pooled fractions used in Figure 3A gels 2, 3, and 8. (C) Total cell extracts were prepared from yeast expressing *MVB12-HA* at different times after treatment with cycloheximide (0, 1, and 2 h) and analyzed by Western blot using anti-HA and anti-Vps23 antibodies. After 2 h of cycloheximide treatment the cells were prepared for gel filtration analysis and the extract loaded onto the column (L) was analyzed by Western blot. The result of this gel filtration analysis is shown in A (gels 8 and 9). (D) The table summarizes the apparent molecular masses of the analyzed proteins relative to the standard proteins thyroglobulin (670 kDa), ferritin (440 kDa), aldolase (158 kDa), albumin (67 kDa), ovalbumin (44 kDa) and myoglobin (17 kDa) (see A).

Mvb12 Seems to Associate with ESCRT-I via Vps37

Deletion of *VPS37* results in the formation of a stable ESCRT-I subcomplex of ~125 kDa that has been shown to contain Vps23 and Vps28 (Figure 3A, gel 6; Kostelansky *et al*., 2006; Teo *et al*., 2006). As shown in Figure 2A, Mvb12 is unstable

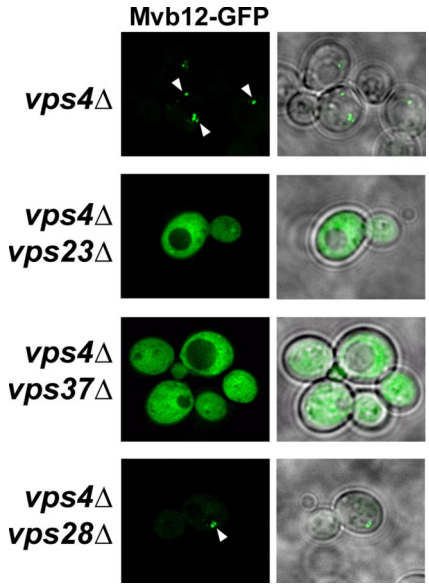

Figure 4. Mvb12 requires Vps23 and Vps37 to localize to endosomes. Fluorescent microscopy of Mvb12-GFP overexpressed from a high-copy plasmid in different mutant backgrounds (arrows indicate class E compartments).

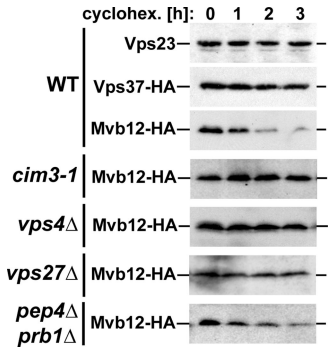

Figure 5. Rapid turnover of Mvb12 by the proteasome depends on a functional MVB pathway. The translation inhibitor cycloheximide (50 mg/l) was added to yeast cultures (t = 0), and samples were taken after addition of the drug at the indicated time points. Cells were lysed using glass beads, and the resulting extracts were analyzed by Western blot for the presence of Vps23, Mvb12-HA, and Vps37-HA.

in this mutant background, suggesting that Mvb12 associates with ESCRT-I via Vps37. To detect Mvb12 in *vps37*Δ, we transformed the mutant strain with a plasmid expressing from the *CPS1* promoter a functional N-terminal fusion of *MVB12* with the HA tag (Supplemental Figure 1). The resulting fusion protein HA-Mvb12, like Mvb12-HA, is unstable in *vps37*Δ, but because of the strong *CPS1* promoter HA-Mvb12 is detectable by Western blot. Cell extract from *vps37*Δ expressing *HA-MVB12* was separated by gel filtration, and Western blot analysis identified small amounts of HA-Mvb12 in the size range of 20 kDa, consistent with the model that Mvb12 requires Vps37 to associate with ESCRT-I (Figure 3A, gel 5). The deletion of *VPS23* resulted in lower but detectable protein levels of Vps37-HA and Mvb12-HA. Analysis of this mutant strain by gel filtration indicated that the remaining pool Vps37-HA and Mvb12-HA form a complex of ~195 kDa in absence of Vps23 (Figure 3A, gel 7, and D). Our result does not exclude the possibility that this 195-kDa complex contains Vps28. However, the crystal structure analysis of ESCRT-I has shown that Vps23 acts as a linker between Vps28 and Vps37, which argues against the presence of Vps28 in 195-kDa complex (Kostelansky *et al.*, 2006; Teo *et al.*, 2006). Together, the results suggested that Vps37 and Mvb12 form a subcomplex.

Further support for the Vps37–Mvb12 interaction was obtained by fluorescence microscopy. To visualize the low levels of Mvb12 in different ESCRT-I mutants, we transformed the mutant strains with a high-copy 2μ plasmid containing *MVB12-GFP* (Figure 4). In cells deleted for *VPS4* the increased levels of Mvb12-GFP localized to class E compartments (Figure 4, arrows) similar to the localization found for Mvb12-GFP expressed at normal levels (Figure 1A). Previous studies have shown that the localization of ESCRT-I to MVBs is mediated by the interaction of Vps23 with Vps27 (Bache *et al.*, 2003; Katzmann *et al.*, 2003). As expected from these studies we found that Mvb12 required Vps23 for proper localization to the endosome (Figure 4, *vps4*Δ*vps23*Δ). The deletion of *VPS28* did not change the endosomal localization of Mvb12-GFP, indicating that Vps28 is not essential for membrane association of Mvb12 (Figure 4, *vps4*Δ*vps28*Δ). In contrast, loss of Vps37 resulted in the redistribution of Mvb12-GFP to the cytoplasm, consistent with our model that Mvb12 binds via Vps37 to ESCRT-I (Figure 4, *vps4*Δ*vps37*Δ).

Mvb12 Is an Unstable ESCRT-I Subunit

We determined the stability of Mvb12-HA in wild-type cells using the translational inhibitor cycloheximide. Cycloheximide was added to yeast cultures and samples were taken immediately (t = 0) and at 1, 2, and 3 h (t = 1 h, 2 h, and 3 h). The cell extracts were analyzed for the presence of Mvb12-HA, Vps23, and Vps37-HA by Western blot (Figure 5). In wild-type cells, Mvb12-HA was rapidly degraded with a half-life of <1 h. Vps37-HA was more stable, having a half-life of 2 to 3 h. In contrast, the amount of Vps23 only changed marginally over the time period of 3 h. Together, the data suggested that compared with other subunits of ESCRT-I, Mvb12 is relatively unstable.

To determine which pathway is responsible for the degradation of Mvb12, we tested the stability of Mvb12-HA in the proteasomal mutant strain *cim3-1* and a strain deleted for two major vacuolar peptidases Pep4 and Prb1. These experiments demonstrated that Mvb12-HA is a stable protein in the proteasomal mutant, but only a minor Mvb12-HA stabilization is observed in the strain deleted for vacuolar peptidases (Figure 5), indicating that the rapid degradation of Mvb12 is primarily dependent on the proteasomal system rather than the vacuole. This result is consistent with the observations by fluorescence microscopy that showed no detectable levels of Mvb12-GFP in the vacuolar lumen (Figure 1A).

The rapid turnover of Mvb12 suggested that ESCRT-I repeatedly exchanges the Mvb12 subunit with a newly synthesized copy. Therefore we expected that blocking translation should result in a shift in size of ESCRT-I over time from 350 to ~170 kDa, the size of ESCRT-I in *mvb12*Δ. To test this prediction, we prepared a cell extract of a wild-type strain expressing Mvb12-HA after 2 h of cycloheximide treatment and analyzed this extract by gel filtration. The Western blot in Figure 3C illustrates that the sample loaded onto the gel filtration column contained at least fivefold less Mvb12-HA than the nontreated sample. In contrast, the amount of Vps23 remained stable during this procedure. The result of the gel filtration analysis indicated that during the cycloheximide treatment a large portion of ESCRT-I shifted to a

smaller molecular mass (Figure 3A, gel 8, and B, gel 12). Vps23 showed a very broad size distribution (170–350 kDa), which is consistent with a mixture of complete ESCRT-I and ESCRT-I missing Mvb12 (Figure 3B). The remaining pool of Mvb12-HA shifted to ~260 kDa after blocking translation for 2 h (Figure 3A, gel 9). It is expected that Mvb12-HA is only present in the larger forms of ESCRT-I that still contain this subunit. However, that Mvb12-HA shifts in size at all suggests that there is more than one subunit of Mvb12 present in each 350-kDa ESCRT-I complex.

The data so far indicated that the ESCRT-I subunit Mvb12 is degraded by the ubiquitin-proteasomal system and that the rate of degradation is faster than observed for other subunits of the ESCRT-I complex. The question remained whether the degradation of Mvb12 is connected to the function of ESCRT-I. Therefore, we analyzed the stability of Mvb12-HA in mutants that impair either the recruitment of ESCRT-I to MVBs (*vps27*Δ) or the dissociation of ESCRT-I from the endosomal membrane (*vps4*Δ). The result shown in Figure 5 indicated that both type of mutants resulted in stabilization of Mvb12-HA, suggesting that the instability of Mvb12 is a function of the transient localization of ESCRT-I to MVBs.

Mvb12 Is Required for Efficient MVB Sorting

To study potential MVB trafficking defects, we transformed the *MVB12* deletion strain with plasmids containing GFP-gene fusions encoding for either CPS fused to GFP (GFP-CPS), Sna3-GFP, Ste2-GFP, or Ste3-GFP. Newly synthesized CPS and Sna3 are transmembrane proteins that are transported through the secretory pathway and via MVBs to the lumen of the vacuole. In contrast to CPS, the sorting of Sna3 into the MVB pathway seems to be independent of ubiquitination (Odorizzi *et al*., 1998; Katzmann *et al*., 2001; Reggiori and Pelham, 2001; Yeo *et al*., 2003). Ste2 and Ste3 are surface receptors that are endocytosed and delivered via the MVB pathway to the vacuolar lumen (Odorizzi *et al*., 1998; Chen and Davis, 2002; Shaw *et al*., 2003). Therefore, in wild-type cells the GFP fluorescence of GFP-CPS and Ste2-GFP is observed by microscopy in the lumen of the vacuole (Figure 6A and Supplemental Figure 2). In contrast, cells defective in the MVB pathway, such as the ESCRT-I mutant *vps23*Δ, accumulate GFP-CPS, Sna3-GFP, Ste2-GFP, and Ste3-GFP in aberrant endosomes (class E compartments; Figure 6A, arrows, and Supplemental Figure 2) and mislocalize cargo proteins to the vacuolar membrane (Figure 6A and Supplemental Figure 2). Surprisingly, the analysis of the *mvb12*Δ trafficking phenotype indicated that these mutant cells have a less severe defect in the MVB sorting pathway (Figure 6A and Supplemental Figure 2). Unlike in *vps23*Δ, *vps28*Δ, and *vps37*Δ, in *MVB12* deletion mutant cells GFP-CPS and Sna3-GFP do not accumulate in class E compartments, and a portion of GFP-CPS and Sna3-GFP is properly localized to the vacuolar lumen. Ste2-GFP and Ste3-GFP showed almost normal trafficking in *mvb12*Δ with only a slight accumulation of the cargo in late endosomes. These data might suggest that the deletion of *MVB12* affects the MVB trafficking of biosynthetic cargo more severely then the trafficking of cargo from the endocytic pathway.

A hallmark of class E *vps* mutants is a partial secretion of vacuolar enzymes caused by the inefficient recycling of the sorting receptor Vps10 (Raymond *et al*., 1992; Cereghino *et al*., 1995; Cooper and Stevens, 1996). This secretion phenotype can be visualized using the reporter carboxypeptidase Y (CPY)-Invertase combined with a colorimetric plate assay (Paravicini *et al*., 1992). Wild-type cells efficiently sort CPY-Invertase to the vacuole and therefore remain white on the assay plate (Figure 6B). Class E *vps* mutants, such as *vps23*Δ,

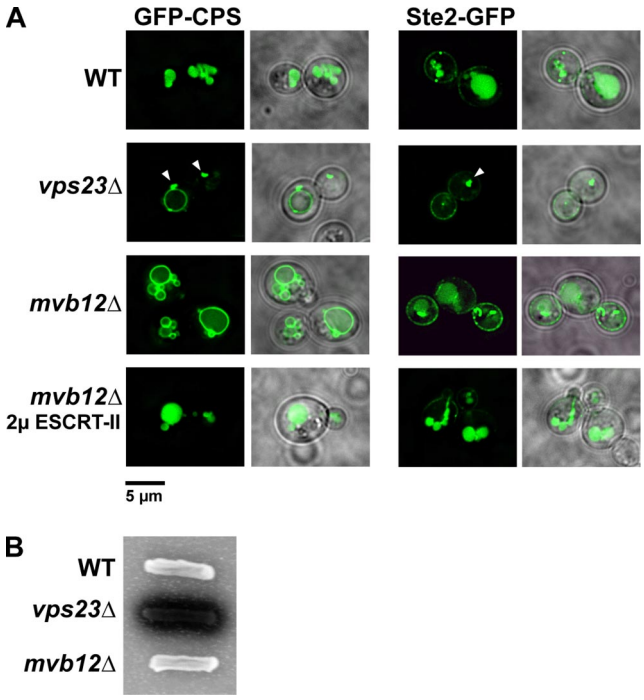

Figure 6. The deletion of *MVB12* results in a mild MVB trafficking phenotype. (A) Strains expressing either GFP-CPS (pGO45) or Ste2-GFP (pCS24) were analyzed by fluorescence microscopy. White arrows indicate class E compartments. ESCRT-II was overexpressed by transforming the cells with the high-copy plasmid pMB175 (2μ ESCRT-II). (B) Invertase plate assay of wild type (BHY10), *vps23*Δ (EEY5-2), and *mvb12*Δ (MCY9).

secrete CPY-Invertase, which results in the colorimetric reaction. In contrast, the *MVB12* deletion strain remained white, indicating that CPY-Invertase was trafficked efficiently to the vacuole in this mutant strain (Figure 6B). Together, the trafficking studies indicated that Mvb12 is not an essential factor for MVB sorting; thus, unlike the other ESCRT-I subunits, Mvb12 does not belong to the group of class E Vps proteins. However, Mvb12 is necessary for the efficient transport of cargo proteins to the lumen of the vacuole.

One possible explanation for the partial MVB trafficking phenotype is that Mvb12 function might be redundant. Therefore, we tested whether overexpression of the ESCRT-I genes *VPS23*, *VPS28*, and *VPS37* could suppress the GFP-CPS trafficking phenotype of an *mvb12*Δ strain. The data of these studies showed no suppression of the GFP-CPS mislocalization (data not shown), suggesting that high levels of the remaining ESCRT-I complex cannot replace the function of Mvb12. However, in similar studies we found that overexpression of the ESCRT-II genes fully suppressed all tested trafficking defects in the *mvb12*Δ mutant (Figure 6A and Supplemental Figure 2). This result is consistent with previous studies that showed suppression of ESCRT-I mutant phenotypes by overexpression of ESCRT-II (Katzmann *et al*., 2001) and therefore is further support of the idea that Mvb12 functions as part of ESCRT-I. However, in contrast to the complete rescue of the *mvb12*Δ phenotype, the mutant phenotype of other ESCRT-I subunits is only partially suppressed by ESCRT-II overexpression (Katzmann *et al*., 2001).

Deletion of MVB12 Affects the Dissociation of ESCRT-I from MVBs

Our studies have shown that deletion of *MVB12* results in the formation of a stable ~170-kDa ESCRT-I complex that is

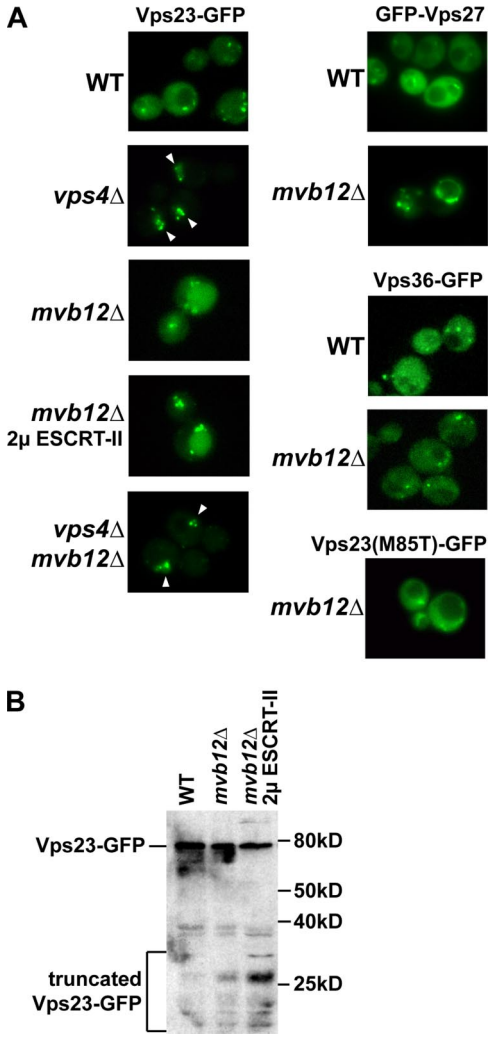

Figure 7. In *mvb12*Δ, ESCRT-I is mislocalized to the vacuolar lumen. (A) Fluorescence microscopy of strains expressing plasmid encoded *GFP-VPS27* (pEE27-4) and *VPS23(M85T)-GFP* (pMB319) or chromosomally integrated *VPS23-GFP* and *VPS36-GFP*. Arrows indicate class E compartments. (B) Western blot analysis using a GFP-specific antibody of extracts from cells expressing chromosomally encoded Vps23-GFP (WT, DKY54; *mvb12*Δ, MBY73; 2μ ESCRT-II, pMB175).

at least partially able to function in the sorting of MVB cargo. To determine whether lack of Mvb12 effects the transient association of ESCRT-I with the endosomal membrane, we studied the localization of the ESCRT-I subunit Vps23 in different strain backgrounds by using a chromosomally integrated functional GFP-tagged *VPS23* fusion protein (Katzmann *et al*., 2001). As shown previously, Vps23-GFP localizes to the cytoplasm and endosomal compartments in wild-type cells and accumulates on class E compartments in cells deleted for *VPS4* (Figure 7A). Interestingly, we found that deleting *MVB12* caused a portion of Vps23-GFP to be transported into the vacuolar lumen (Figure 7A). This transport required the MVB trafficking pathway because the deletion of *VPS4* in *mvb12*Δ prevented the vacuolar localization of Vps23-GFP and resulted in endosomal accumulation of the fusion protein similar as observed in the *vps4*Δ strain. Deletion of *MVB12* did not effect Vps36-GFP localization (Figure 7A) but caused GFP-Vps27 to accumulate on large structures adjacent to the vacuole that most likely are late endosomal compartments (Figure 7A). No accumulation of GFP-Vps27 was observed inside the vacuole. Similar redistribution of Vps27 has been observed in other ESCRT-I mutants (Katzmann *et al*., 2003). Interestingly, a mutation in the UEV domain of Vps23 (methionine 85 to threonine, M85T) that previously had been shown to impair ubiquitin binding (Katzmann *et al*., 2001) resulted in loss of vacuolar localization of Vps23-GFP in *mvb12*Δ cells (Figure 7A). Because these cells expressed wild-type Vps23 in addition to Vps23(M85T)-GFP, the observed effect was not due to a defect in MVB trafficking. Together, these results suggest that binding to ubiquitinated cargo is necessary for the delivery of Vps23-GFP into the vacuolar lumen of *mvb12*Δ cells.

We have shown that overexpression of ESCRT-II suppresses the trafficking defect of an *MVB12* deletion (Figure 6A). In contrast, we found that overexpression of ESCRT-II does not suppress the vacuolar localization of Vps23-GFP, but instead increases the severity of this mislocalization phenotype (Figure 7A). This result suggested that the increased efficiency of MVB sorting in the ESCRT-II overexpression strain also results in an increased delivery of ESCRT-I to the vacuolar lumen. The findings of these microscopy studies are further supported by anti-GFP Western blot analysis of extracts from wild-type, *mvb12*Δ-, and *mvb12*Δ-overexpressing ESCRT-II cells, each containing the chromosomally integrated *VPS23-GFP* fusion (Figure 7B). In comparison with wild type cells, *mvb12*Δ cells contained an increased amount of truncated Vps23-GFP, which was even further increased when ESCRT-II was overexpressed. This increase in truncated Vps23-GFP mirrors the increased GFP signal observed by microscopy in the lumen of the vacuole, suggesting that the truncated Vps23-GFP species represent degradation intermediates of vacuolar Vps23-GFP. As expected, the most prevalent degradation products are in the size range of GFP protein, which is generally a very stable protein (~25 kDa). Furthermore, Western blot analysis showed that the amount of full-length Vps23-GFP did not change dramatically in cells deleted for MVB12, suggesting that the delivery of Vps23-GFP to the vacuole is inefficient and does not result in the depletion of cytoplasmic Vps23-GFP (Figure 7B). Because GFP is a very stable protein that is able to persist in the vacuole for an extended time period, the strong GFP signal observed by microscopy in the vacuolar lumen of *mvb12*Δ expressing Vps23-GFP (Figure 7A) is probably due to GFP accumulation over a long period rather than rapid vacuolar delivery of Vps23-GFP.

DISCUSSION

The ESCRT-I protein complex is part of the protein machinery that executes endosomal (MVB) sorting of ubiquitinated cargo and formation of MVB vesicles (for review, see Hurley and Emr, 2006). ESCRT-I localizes to the cytoplasm and is transiently recruited to the endosomal membrane. This recruitment step is mediated by the interaction of ESCRT-I with endosomal localized Vps27 (Bilodeau *et al*., 2003; Katzmann *et al*., 2003). On the endosome, ESCRT-I and Vps27 bind to monoubiquitinated cargo to initiate their sorting into MVB vesicles (Katzmann *et al*., 2001; Bilodeau *et al*., 2002). Subsequently, ESCRT-I interacts with ESCRT-II, a protein complex that functions in the formation of ESCRT-III (Babst *et al*., 2002a,b; Teo *et al*., 2006). Finally, ESCRT-I is released from the MVB membrane and recycled for further rounds of sorting.

In this study, we have found evidence for the presence of a forth subunit of yeast ESCRT-I, called Mvb12 (SGD:

YGR206w). Immunoprecipitation and affinity purification experiments demonstrated a physical interaction between Mvb12 and ESCRT-I. Gel filtration analysis of yeast cell extract indicate that Mvb12 has a native molecular mass similar to that of ESCRT-I (350 kDa) and that deletion of *MVB12* causes a shift in size of ESCRT-I from 350 to ~170 kDa. Furthermore, we observed that Mvb12 is unstable in cells lacking any of the ESCRT-I subunits. Finally, Mvb12 colocalizes with ESCRT-I and the subcellular distribution of Mvb12 is consistent with the published transient MVB association of ESCRT-I (Katzmann *et al*., 2001). Previous studies have shown that native ESCRT-I has an apparent molecular mass of 350 kDa and is composed of the class E Vps proteins Vps23, Vps28, and Vps37 (Babst *et al*., 2000; Katzmann *et al*., 2001). Recent crystal structure analysis suggested that these three subunits form a trimeric complex with a 1:1:1 stoichiometry (Kostelansky *et al*., 2006; Teo *et al*., 2006). Because only a substructure of ESCRT-I has been analyzed by crystallography, the exact composition of the in vivo observed 350-kDa complex remains unknown.

The gel filtration data of different ESCRT-I mutants are consistent with a model in which Mvb12 interacts with ESCRT-I via the Vps37 subunit. However, the number of Mvb12 subunits present in each 350-kDa ESCRT-I complex is not clear. Deletion of *MVB12* resulted in a shift in size of ESCRT-I from ~350 to ~170 kDa, suggesting that Mvb12 might promote dimerization of a Vps23-Vps28-Vps37 complex or that ESCRT-I contains at least 10 Mvb12 subunits. Finally, we cannot exclude the possibility that ESCRT-I contains additional not yet identified subunits that require Mvb12 to interact with ESCRT-I.

Both gel filtration analysis and immunoprecipitation experiments indicate that Mvb12 is tightly associated with ESCRT-I. Surprisingly, in wild-type cells we observed a rapid proteasome-dependent turnover of Mvb12, resulting in a half-life of Mvb12 that is much shorter then the half-life of other ESCRT-I subunits. As a consequence, when new protein synthesis was blocked, the ESCRT-I complex gradually shifted in size from ~350 to ~170 kDa. This result indicated that during the lifetime of an ESCRT-I complex, Mvb12 is repeatedly degraded and replaced by newly synthesized Mvb12 subunits. Interestingly, Mvb12 degradation was found to be dependent on the transient localization of ESCRT-I to the endosome. Loss of either the ESCRT-I recruiting factor Vps27 or the recycling factor Vps4 resulted in the stabilization of Mvb12. This result suggested that the rapid degradation of Mvb12 is a consequence of ESCRT-I function on the endosome.

Loss of function of Vps23, Vps28, or Vps37 resulted in a complete block of the MVB pathway (Babst *et al*., 2000; Katzmann *et al*., 2001). In contrast, deletion of *MVB12* only partially affects the transport of MVB cargoes to the vacuolar lumen, indicating that Mvb12 is not an essential factor for ESCRT-I function. We found that the trafficking defects in *mvb12*Δ are more severe for cargo of the biosynthetic pathway (e.g., CPS and Sna3) than for endocytic cargo (e.g., Ste2 and Ste3). It is not clear whether this difference indicates the presence of two partially separate MVB pathways, a biosynthetic and an endocytic pathway, or whether it reflects cargo specificity of Mvb12 function.

In *mvb12*Δ cells, ESCRT-I localizes to endosomal compartments and the lumen of the vacuole, indicating that Mvb12 is not required for the recruitment of ESCRT-I to MVBs but instead seems to be play a role in the dissociation of ESCRT-I from the endosome after the function of ESCRT-I in cargo sorting is completed. However, the delivery of ESCRT-I into the MVB pathway in *MVB12*-deleted cells is not efficient enough to deplete the cells of ESCRT-I and is not the cause of the MVB-trafficking defects observed in *mvb12*Δ. Consistent with the role of ESCRT-II in cargo sorting downstream of ESCRT-I, we found that overexpression of ESCRT-II suppressed the trafficking phenotype of *mvb12*Δ. In contrast, the mislocalization of mutant ESCRT-I to the vacuolar lumen was enhanced by the overexpression of ESCRT-II, suggesting that ESCRT-II overexpression increased MVB trafficking not only of cargo but also of ESCRT-I.

Deletion of *MVB12* caused ESCRT-I to be targeted to the vacuolar lumen, but it did not result in vacuolar localization of Vps27 or ESCRT-II. This observation suggests that the defect in ESCRT-I recycling in *mvb12*Δ is not a result of ESCRT-I not being able to break the interactions with other ESCRT machinery, but rather it is caused by maintaining (prolonging) the interaction with ubiquitinated cargo. This model is supported by the observation that a ubiquitin-binding mutant of Vps23 does not get delivered to the vacuolar lumen in an *MVB12* deletion strain. Several proteins of the ESCRT machinery contain ubiquitin-binding domains that recognize a similar ubiquitin surface (for review, see Hurley and Emr, 2006). It has therefore been speculated that ubiquitinated cargo might be handed over from one ubiquitin-binding protein complex to the next (e.g., from ESCRT-I to ESCRT-II). However, the *mvb12*Δ phenotype suggests that cargo is sorted into the MVB pathway even when it remains bound to ESCRT-I. Furthermore, we observed that overexpression of ESCRT-II in *mvb12*Δ results in increased transport of both cargo and ESCRT-I to the vacuolar lumen, indicating that ESCRT-II does not compete with ESCRT-I for cargo. Together, our data are most consistent with a model in which sorting of ESCRT-I-bound cargo into MVB vesicles does not require the release of cargo from ESCRT-I and subsequent interaction with ESCRT-II.

Although Mvb12 plays an important role in the function of yeast ESCRT-I, the protein sequence of Mvb12 is evolutionarily poorly conserved. As a consequence, convincing Mvb12 homologues are only found among other fungal species. However, lack of sequence homology does not rule out the possibility that functional homologues of Mvb12 also exist in higher eukaryotes. Similar to Mvb12, very little sequence conservation is observed between Vps37 proteins from different species. Considering the high structural and functional conservation of other parts of the ESCRT machinery it is unlikely that this sequence diversity among different species reflects a difference in the function of ESCRT-I.

The current MVB sorting model suggests that after recruitment to the MVB, ESCRT-I binds to ubiquitinated cargo and to ESCRT-II, which initiates the formation of ESCRT-III. At some point, either during ESCRT-III formation or the dissociation of ESCRT-III by Vps4, the ESCRT-I complex dissociates from the ESCRT machinery and is released to the cytoplasm for further rounds of sorting. Our data suggest that loss of Mvb12 affects a step in ESCRT-I function after the endosomal recruitment and binding of cargo. This defect results in inefficient cargo sorting and in inefficient dissociation of ESCRT-I from the MVB. One possible function for Mvb12 could be to interact with other components of the ESCRT machinery, thereby regulating and coordinating the transient interactions of ESCRT-I with cargo and machinery. Without Mvb12, ESCRT-I might not properly activate the downstream ESCRT-II complex, which might affect the release of ESCRT-I from the ubiquitinated cargo. The rapid degradation of Mvb12 observed in wild-type cells might be a result of the ESCRT-I release from the MVB. During the release reaction, Mvb12 might dissociate from the complex and be degraded by the proteasomal system. It will be interesting to test whether

the observed modification of endosomal Mvb12 plays a role in regulating the interaction between ESCRT-I, ubiquitinated cargo, and other parts of the ESCRT machinery.

ACKNOWLEDGMENTS

We thank Tamara Darsow for critical reading of the manuscript. We thank Dan Gottschling for providing the *cim3-1* strain. This work has been supported by grant R01 GM-074171-01 A1 from the National Institute of Health and by a Funding Incentive Seed Grant (project 51003083) from the University of Utah.

REFERENCES

Babst, M. (2005). A protein's final ESCRT. Traffic *6*, 2–9.

Babst, M., Katzmann, D. J., Estepa-Sabal, E. J., Meerloo, T., and Emr, S. D. (2002a). Escrt-III: an endosome-associated heterooligomeric protein complex required for mvb sorting. Dev. Cell *3*, 271–282.

Babst, M., Katzmann, D. J., Snyder, W. B., Wendland, B., and Emr, S. D. (2002b). Endosome-associated complex, ESCRT-II, recruits transport machinery for protein sorting at the multivesicular body. Dev. Cell *3*, 283–289.

Babst, M., Odorizzi, G., Estepa, E. J., and Emr, S. D. (2000). Mammalian tumor susceptibility gene 101 (TSG101) and the yeast homologue, Vps23p, both function in late endosomal trafficking. Traffic *1*, 248–258.

Babst, M., Sato, T. K., Banta, L. M., and Emr, S. D. (1997). Endosomal transport function in yeast requires a novel AAA-type ATPase, Vps4p. EMBO J. *16*, 1820–1831.

Babst, M., Wendland, B., Estepa, E. J., and Emr, S. D. (1998). The Vps4p AAA ATPase regulates membrane association of a Vps protein complex required for normal endosome function. EMBO J. *17*, 2982–2993.

Bache, K. G., Brech, A., Mehlum, A., and Stenmark, H. (2003). Hrs regulates multivesicular body formation via ESCRT recruitment to endosomes. J. Cell Biol. *162*, 435–442.

Bilodeau, P. S., Urbanowski, J. L., Winistorfer, S. C., and Piper, R. C. (2002). The Vps27p Hse1p complex binds ubiquitin and mediates endosomal protein sorting. Nat. Cell Biol. *4*, 534–539.

Bilodeau, P. S., Winistorfer, S. C., Kearney, W. R., Robertson, A. D., and Piper, R. C. (2003). Vps27-Hse1 and ESCRT-I complexes cooperate to increase efficiency of sorting ubiquitinated proteins at the endosome. J. Cell Biol. *163*, 237–243.

Cereghino, J. L., Marcusson, E. G., and Emr, S. D. (1995). The cytoplasmic tail domain of the vacuolar sorting receptor Vps10p and a subset of VPS gene products regulate receptor stability, function and localization. Mol. Biol. Cell *6*, 1089–1102.

Ceresa, B. P., and Schmid, S. L. (2000). Regulation of signal transduction by endocytosis. Curr. Opin. Cell Biol. *12*, 204–210.

Chen, L., and Davis, N. G. (2002). Ubiquitin-independent entry into the yeast recycling pathway. Traffic *3*, 110–123.

Christianson, T. W., Sikorski, R. S., Dante, M., Shero, J. H., and Hieter, P. (1992). Multifunctional yeast high-copy-number shuttle vectors. Gene *110*, 119–122.

Cooper, A. A., and Stevens, T. H. (1996). Vps10p cycles between the late-Golgi and prevacuolar compartments in its function as the sorting receptor for multiple yeast vacuolar hydrolases. J. Cell Biol. *133*, 529–541.

Di Fiore, P. P., and Gill, G. N. (1999). Endocytosis and mitogenic signaling. Curr. Opin. Cell Biol. *11*, 483–488.

Gruenberg, J., and Stenmark, H. (2004). The biogenesis of multivesicular endosomes. Nat. Rev. Mol. Cell Biol. *5*, 317–323.

Hirano, S., Kawasaki, M., Ura, H., Kato, R., Raiborg, C., Stenmark, H., and Wakatsuki, S. (2006). Double-sided ubiquitin binding of Hrs-UIM in endosomal protein sorting. Nat. Struct. Mol. Biol. *13*, 272–277.

Huh, W. K., Falvo, J. V., Gerke, L. C., Carroll, A. S., Howson, R. W., Weissman, J. S., and O'Shea, E. K. (2003). Global analysis of protein localization in budding yeast. Nature *425*, 686–691.

Hurley, J. H., and Emr, S. D. (2006). The ESCRT complexes: structure and mechanism of a membrane-trafficking network. Annu. Rev. Biophys. Biomol. Struct. *35*, 277–298.

Ito, H., Fukuda, Y., Murata, K., and Kimura, A. (1983). Transformation of intact yeast cells treated with alkali cations. J. Bacteriol. *153*, 163–168.

Katzmann, D. J., Babst, M., and Emr, S. D. (2001). Ubiquitin-dependent sorting into the multivesicular body pathway requires the function of a conserved endosomal protein sorting complex, ESCRT-I. Cell *106*, 145–155.

Katzmann, D. J., Odorizzi, G., and Emr, S. D. (2002). Receptor downregulation and multivesicular-body sorting. Nat. Rev. Mol. Cell Biol. *3*, 893–905.

Katzmann, D. J., Stefan, C. J., Babst, M., and Emr, S. D. (2003). Vps27 recruits ESCRT machinery to endosomes during MVB sorting. J. Cell Biol. *162*, 413–423.

Kostelansky, M. S., Sun, J., Lee, S., Kim, J., Ghirlando, R., Hierro, A., Emr, S. D., and Hurley, J. H. (2006). Structural and functional organization of the ESCRT-I trafficking complex. Cell *125*, 113–126.

Luhtala, N., and Odorizzi, G. (2004). Bro1 coordinates deubiquitination in the multivesicular body pathway by recruiting Doa4 to endosomes. J. Cell Biol. *166*, 717–729.

Murk, J. L., Stoorvogel, W., Kleijmeer, M. J., and Geuze, H. J. (2002). The plasticity of multivesicular bodies and the regulation of antigen presentation. Semin. Cell Dev. Biol. *13*, 303–311.

Odorizzi, G., Babst, M., and Emr, S. D. (1998). Fab1p PtdIns(3)P 5-kinase function essential for protein sorting in the multivesicular body. Cell *95*, 847–858.

Paravicini, G., Horazdovsky, B. F., and Emr, S. D. (1992). Alternative pathways for the sorting of soluble vacuolar proteins in yeast: a *vps35* null mutant missorts and secretes only a subset of vacuolar hydrolases. Mol. Biol. Cell *3*, 415–427.

Pornillos, O., Alam, S. L., Rich, R. L., Myszka, D. G., Davis, D. R., and Sundquist, W. I. (2002). Structure and functional interactions of the Tsg101 UEV domain. EMBO J. *21*, 2397–2406.

Raymond, C. K., Howald-Stevenson, I., Vater, C. A., and Stevens, T. H. (1992). Morphological classification of the yeast vacuolar protein sorting mutants: evidence for a prevacuolar compartment in class E *vps* mutants. Mol. Biol. Cell *3*, 1389–1402.

Reggiori, F., and Pelham, H. R. (2001). Sorting of proteins into multivesicular bodies: ubiquitin-dependent and -independent targeting. EMBO J. *20*, 5176–5186.

Robinson, J. S., Klionsky, D. J., Banta, L. M., and Emr, S. D. (1988). Protein sorting in *Saccharomyces cerevisiae*: isolation of mutants defective in the delivery and processing of multiple vacuolar hydrolases. Mol. Cell Biol. *8*, 4936–4948.

Rothman, J. H., and Stevens, T. H. (1986). Protein sorting in yeast: mutants defective in vacuole biogenesis mislocalize vacuolar proteins into the late secretory pathway. Cell *47*, 1041–1051.

Sambrook, J., Fritsch, E. F., and Maniatis, T. (1989). Molecular Cloning. A Laboratory Manual, 2nd ed., Cold Spring Harbor, NY: Cold Spring Harbor Laboratory Press.

Shaw, J. D., Hama, H., Sohrabi, F., DeWald, D. B., and Wendland, B. (2003). PtdIns(3,5)P2 is required for delivery of endocytic cargo into the multivesicular body. Traffic *4*, 479–490.

Sherman, F., Fink, G. R., and Lawrence, L. W. (1979). Methods in Yeast Genetics: A Laboratory Manual, Cold Spring Harbor, NY: Cold Spring Harbor Laboratory Press.

Shih, S. C., Katzmann, D. J., Schnell, J. D., Sutanto, M., Emr, S. D., and Hicke, L. (2002). Epsins and Vps27p/Hrs contain ubiquitin-binding domains that function in receptor endocytosis. Nat. Cell Biol. *4*, 389–393.

Sundquist, W. I., Schubert, H. L., Kelly, B. N., Hill, G. C., Holton, J. M., and Hill, C. P. (2004). Ubiquitin recognition by the human TSG101 protein. Mol. Cell *13*, 783–789.

Swanson, K. A., Kang, R. S., Stamenova, S. D., Hicke, L., and Radhakrishnan, I. (2003). Solution structure of Vps27 UIM-ubiquitin complex important for endosomal sorting and receptor downregulation. EMBO J. *22*, 4597–4606.

Teo, H., Gill, D. J., Sun, J., Perisic, O., Veprintsev, D. B., Vallis, Y., Emr, S. D., and Williams, R. L. (2006). ESCRT-I core and ESCRT-II GLUE domain structures reveal role for GLUE in linking to ESCRT-I and membranes. Cell *125*, 99–111.

Teo, H., Veprintsev, D. B., and Williams, R. L. (2004). Structural insights into endosomal sorting complex required for transport (ESCRT-I) recognition of ubiquitinated proteins. J. Biol. Chem. *279*, 28689–28696.

Thompson, B. J., Mathieu, J., Sung, H. H., Loeser, E., Rorth, P., and Cohen, S. M. (2005). Tumor suppressor properties of the ESCRT-II complex component Vps25 in *Drosophila*. Dev. Cell *9*, 711–720.

Vaccari, T., and Bilder, D. (2005). The *Drosophila* tumor suppressor vps25 prevents nonautonomous overproliferation by regulating notch trafficking. Dev. Cell *9*, 687–698.

Yeo, S. C., *et al*. (2003). Vps20p and Vta1p interact with Vps4p and function in multivesicular body sorting and endosomal transport in *Saccharomyces cerevisiae*. J. Cell Sci. *116*, 3957–3970.